STEM CELLS AND DEVELOPMENT
Volume 22, Number 11, 2013

DOI: 10.1089/scd.2012.0247

Molecular and Functional Evidence of HCN4 and Caveolin-3 Interaction During Cardiomyocyte Differentiation from Human Embryonic Stem Cells

Alexis Bosman,[1] Laura Sartiani,[2] Valentina Spinelli,[1,2] Martina Del Lungo,[2] Francesca Stillitano,[2] Daniele Nosi,[3] Alessandro Mugelli,[2] Elisabetta Cerbai,[2] and Marisa Jaconi[1]

Maturation of human embryonic stem cell-derived cardiomyocytes (hESC-CM) is accompanied by changes in ion channel expression, with relevant electrophysiological consequences. In rodent CM, the properties of hyperpolarization-activated cyclic nucleotide-gated channel (HCN)4, a major f-channel isoform, depends on the association with caveolin-3 (Cav3). To date, no information exists on changes in Cav3 expression and its associative relationship with HCN4 upon hESC-CM maturation. We hypothesize that Cav3 expression and its compartmentalization with HCN4 channels during hESC-CM maturation accounts for the progression of f-current properties toward adult phenotypes. To address this, hESC were differentiated into spontaneously beating CM and examined at ~30, ~60, and ~110 days of differentiation. Human adult and fetal CM served as references. HCN4 and Cav3 expression and localization were analyzed by real time PCR and immunocyto/histochemistry. F-current was measured in patch-clamped single cells. HCN4 and Cav3 co-localize in adult human atrial and ventricular CM, but not in fetal CM. Proteins and mRNA for Cav3 were not detected in undifferentiated hESC, but expression increased during hESC-CM maturation. At 110 days, HCN4 appeared to be colocalized with Cav3. Voltage-dependent activation of the f-current was significantly more positive in fetal CM and 60-day hESC-CM (midpoint activation, $V_{1/2}$, ~ −82 mV) than in 110-day hESC-CM or adult CM ($V_{1/2}$ ~ −100 mV). In the latter cells, caveolae disruption reversed voltage dependence toward a more positive or an immature phenotype, with $V_{1/2}$ at −75 mV, while in fetal CM voltage dependence was not affected. Our data show, for the first time, a developmental change in HCN4-Cav3 association in hESC-CM. Cav3 expression and its association with ionic channels likely represent a crucial step of cardiac maturation.

Introduction

Caveolin-3 (Cav3) is a constituent protein of the sarcolemma, typically present in cardiac and skeletal muscles. It is abundantly expressed in caveolae—a subset of morphologically distinct membrane lipid rafts—where it is colocalized with several membrane proteins, including ion channels [1]. The Cav3-channel interaction is known to affect the intrinsic biophysical properties of ion currents and of their susceptibility to modulating signals [1]. An interesting paradigm of such an association and its functional consequences takes place in rabbit sinoatrial node (SAN) cells, where Cav3 colocalizes with the type-4 isoform of the Hyperpolarization-activated Cyclic Nucleotide-gated channel (HCN)4, thus affecting current biophysical properties, especially its activation dependence [2,3]. To date, no data exist concerning the molecular expression/localization of Cav3 in human embryonic stem cell-derived cardiomyocytes (hESC-CM), a suitable model for studying the developmental changes in the electrophysiological properties of cardiac cells.

Our previous work demonstrated the abundant expression of HCN4 channels in hESC-CM starting from very early stages of differentiation, including, surprisingly, in undifferentiated hESC. Concomitantly, at a functional level, an I_f-like current is detected, whose biophysical features vary during in vitro maturation of hESC-CM [4]. At the time of this study, we speculated that changes in molecular attributes, such as the relative amount of HCN isoforms, and/or modulation by other membrane proteins coassembling with the HCN channels may contribute to this phenomenon.

[1]Department of Pathology and Immunology, Faculty of Medicine, Geneva University, Geneva, Switzerland.
[2]Centro Interuniversitario di Medicina Molecolare e Biofisica Applicata, University of Firenze, Firenze, Italy.
[3]Dipartimento di Anatomia, Istologia e Medicina Legale, University of Firenze, Firenze, Italy.

We reasoned that, due to its widespread expression throughout hESC-CM differentiation and maturation, HCN4 might represent a suitable candidate to study changes in the Cav3-protein interaction during in vitro maturation toward the adult cardiac phenotype. In fact, in the human heart, HCN4/I_f is constitutively present in the human adult atrial (hAA) and ventricular (hAV) CM [5,6], although an association with Cav3 has never been investigated.

In the present study, we have examined the expression/localization of cardiac HCN4 and Cav3 in undifferentiated hESC and hESC-CM at different stages, to ascertain the differences in expression of the f-channels according to the developmental age and maturity; at the same time, we performed electrophysiological measurements to determine I_f properties. hAA and hAV CM and human fetal (hF) CM were used as references.

Materials and Methods

Cell culture

All chemicals were obtained from Gibco BRL unless otherwise indicated. All cultures were kept in a humidified incubator at 37°C and maintained with a 5% CO_2 atmosphere. Feeder cells were commercially available human foreskin fibroblasts (HFF) (ATCC). HFF cultures were mitotically inactivated using gamma irradiation (45 Gy), and plated onto 6-well culture dishes (Becton Dickinson AG) at a density of 2.5×10^4 cells/cm^2. The feeder cell culture medium comprised of the high glucose Dulbecco's modified Eagle medium (DMEM) + Glutamax with the addition of 50 U/mL penicillin and 50 mg/mL streptomycin and 10% fetal calf serum.

The hESC line H1 from the WiCell Research Institute was cultured as described previously [4]. Briefly, cells were cultured in the stem cell medium consisting of the DMEM/F12 with 2 mM glutamine, 50 U/mL penicillin and 50 mg/mL streptomycin, 1× minimal essential medium (MEM) amino acids, 0.1 mM β-mercaptoethanol (Sigma-Aldrich GmbH), 20% Knock-out Serum Replacement (KSR), and 4 ng/mL of the basic fibroblast growth factor (R&D Systems) on irradiated HFF. After collagenase IV treatment for 10–15 min at 37°C followed by mechanical dissociation, colonies of hESC were passaged once a week at a ratio of 1:3 to 1:5 onto mitotically inactivated HFF.

hF heart cells were isolated from fetal hearts obtained from aborted material (gestational weeks 9–12), upon the validated informed consent procedure and prior approval by the regional ethics committee in Geneva (protocol authorization #02-088, Gyn-Ob 02-007) and the local ethics committee in Florence (protocol #6783-04, AziendaOspedalieraCareggi, 1-02-2002). The investigation conforms to the principles outlined in the Declaration of Helsinki.

For tissue culture, the cardiac material was minced into small pieces and digested in 3–5 mL of a buffer solution (containing [in mmol/L] NaCl, 116; HEPES, 20; NaH_2PO_4, 1; glucose, 5.5; KCl, 5.4; $MgSO_4$, 0.8; pH 7.35) containing collagenase (Collagenase type IV, Worthington 1 mg/mL) and pancreatin (0.15 mg/mL, Life Technologies), during continuous stirring for 15 min at 37°C in an incubator at humidified atmosphere containing 5% CO_2. The supernatant fraction of cells was collected, while the remaining tissue fragments in the supernatant were repeatedly digested in a fresh enzyme solution. The supernatant was saved every 15 min until all pieces were mostly dissociated. The obtained cells were washed by centrifugation at 140*g* for 5 min, resuspended in a culture medium composed of knockout (KO)-DMEM with 2 mM glutamine, 50 U/mL penicillin and 50 mg/mL streptomycin, 1×MEM amino acids, 0.1 mM β-mercaptoethanol (Sigma-Aldrich GmbH), 20% fetal bovine serum (FBS) (Hyclone) and seeded onto gelatin-coated glass coverslips.

Embryoid body formation and culture

Differentiation media 1 (DM1) was comprised of the KO-DMEM with 2 mM glutamine, 50 U/mL penicillin and 50 mg/mL streptomycin, 1×MEM amino acids, 0.1 mM β-mercaptoethanol (Sigma-Aldrich GmbH), and 20% KSR. Differentiation media 2 (DM2) was comprised of the KO-DMEM with 2 mM glutamine, 50 U/mL penicillin and 50 mg/mL streptomycin, 1×MEM amino acids, 0.1 mM β-mercaptoethanol (Sigma-Aldrich GmbH), and 20% FBS (Hyclone). Embryoid bodies (EBs) were prepared as previously described [7]. Briefly, 60%–80% confluent hESC cultures at passages 40–70 were treated with collagenase type IV for 15–20 min at 37°C and rinsed once with phosphate-buffered saline (PBS) (Ca^{2+} and Mg^{2+} free). Colonies were scraped gently in DM1, transferred to 15-mL polystyrene tubes, and allowed to sediment by gravity for 5–10 min. A supernatant containing most of the irradiated HFF was discarded. Cell clumps were then transferred to Costar Ultra-Low attachment 6-well plates (Corning) at a 2:1 ratio. After 2 days, the medium was changed with DM1, and then at day 4, ~3 EB were transferred to each well of a gelatin-coated 24-well plate (Falcon, BD Biosciences). The medium was changed every 2–3 days with DM2. The appearance of beating areas was monitored using an inverted microscope (Eclipse TE300, Nikon) that was equipped with a Coolpix 995 camera (Nikon) to take phase-contrast pictures and movies.

Cell isolation from EBs and fetal ventricles used for electrophysiological recordings

Beating EBs were dissected using a microscalpel under an inverted microscope and rinsed with PBS containing 0.9 mM $CaCl_2$. hF ventricles were minced into small pieces in PBS supplemented with 0.9 mM $CaCl_2$. Digestion was performed with collagenase B (Roche Applied Science) in PBS (1–2 mg/mL) supplemented with 30 μM $CaCl_2$ for 15–20 min at 37°C. Dissociated cells were plated on gelatin-coated dishes in the DM2 medium and used within 2 days.

Isolation of single human atrial or ventricular myocytes

For all experiments involving human tissue, each investigation conforms to the principles outlined in the Declaration of Helsinki and had been approved by the local ethics committee in Florence (No. 2006/0023797). Atrial CM were isolated from human atrial appendages routinely excised from the heart of patients undergoing a coronary bypass surgery. Ventricular cells were isolated from the septal tissue of a patient affected by hypertrophic cardiomyopathy and undergoing septalmyectomy. The specimens were transported to the laboratory in a cold transport saline solution, cut into small blocks, and then digested in a tissue

dissociation vessel at 37°C, using collagenase type IV (Sigma) and protease type XXIV (Sigma) [8]. After isolation, the cells were collected in tubes with the Kraft-Bruhe solution (see "Solutions and chemicals") for ½ h. Cells were centrifuged at 700 rpm for 5 min and the pellet was resuspended in the Tyrode solution (see "Solutions and chemicals") for electrophysiological recordings or in the new Kraft-Bruhe solution for immunocytochemistry.

Immunocytochemistry

Beating clusters derived from hESC and hF heart cells were grown on gelatin-coated coverslips. Adult atrial and ventricular CM were seeded on laminin-coated dishes in the Kraft-Bruhe solution. Before staining, coverslips were rinsed once with PBS, fixed for 15 min with 4% paraformaldeyde, rinsed 3 times with PBS, and permeabilized with 0.3% Triton X-100 in PBS for 10 min. Cells were then rinsed 3 times with PBS for 5 min and blocked with 1% bovine serum albumin (BSA) in PBS for 10 min. Primary antibodies at appropriate dilutions were incubated for 1 h at 37°C in PBS containing 0.1% Tween-20 and 1% BSA. Before incubation with secondary antibodies, cells were blocked again for 10 min with 10% BSA in PBS. Secondary antibodies at appropriate dilutions were incubated for 1 h at 37°C in PBS containing 0.1% Tween-20 and 1% BSA. Cells were then washed with 0.1% Tween-20 in PBS containing 4′,6-diamidino-2-phenylindole (DAPI) for 10 min. Finally, cells were washed 2 more times with 0.1% Tween 20 in PBS for 10 min, and then mounted onto glass slides with Mowiol and left overnight in the dark at room temperature before observation under the microscope. Atrial and ventricular CM were mounted with the HardSet Mounting Medium containing DAPI (Vectashield) The following primary antibodies were used: mouse monoclonal anti-Oct-4 (Santa Cruz Biotechnology); mouse monoclonal anti-α-actinin (Sigma); mouse anti-Caveolin-3 (BD Biosciences); rabbit anti-HCN-4 (Alomone), rat anti-HCN-4 (Abcam); goat anti-Nkx-2.5 (Santa Cruz). The following secondary antibodies were used: goat anti-mouse Alexa 568 (Molecular Probes); goat anti-rabbit Alexa 568 (Molecular Probes); rabbit anti-goat IgG-FITC (Sigma); goat anti-mouse Alexa Fluor 594 (Invitrogen) and goat anti-rat Alexa Fluor 488 (Invitrogen) for atrial cells; anti-mouse Fi2000 490 (Vector Laboratories) and goat anti-rat Alexa Fluor 594 (Invitrogen) for ventricular cells. Images were visualized with a Zeiss axiophot microscope (Carl Zeiss) equipped with an Axiocam camera (Carl Zeiss); confocal images were obtained using the LSM 510 laser scanning confocal microscope (Carl Zeiss). For atrial and ventricular cells, images were obtained with a Leica TCSSP5 and a Leica SP2-AOBS confocal microscope. 3D images were created using the image analysis program, Imaris.

Immunohistochemistry

Beating clusters derived from hESC and hF heart (~12 weeks) were embedded in paraffin and sectioned into 3-μM slices and placed on glass slides, as reported elsewhere. Slices were deparaffinized, and then rehydrated and unmasking of the epitopes was performed using a pressure cooker in the citrate buffer. After blocking with 10% BSA in PBS for 1 h, primary antibodies at appropriate dilutions were incubated for 1 h at room temperature, and then stained as per the DakoEnVision™ Detection Systems Peroxidase/DAB Kit (see manufacturer's instructions).

RNA extraction and real-time PCR (qPCR)

Total RNA was extracted from cells with the TRIZOL reagent (Invitrogen AG) according to the manufacturer's instructions. 1 μg of total RNA was converted to cDNA with M-MLV Reverse Transcriptase (Invitrogen) using random primers in a 20 μL reaction incubated at 25°C for 10 min followed by 50 min at 37°C and 15 min at 70°C. Volume was adjusted to 50 μL. qPCR was performed with 1 μL of cDNA in a total volume of 25 μL using SYBR green with the ABI Prism 7900 HT detection system (Applied Biosystems). Primers sequences used were as follows:

GusB-F: CCACCAGGGACCATCCAAT; R: AGTCAAAA TATGTGTTCTGGACAAAGTAA

HCN1-F: TCATTCAACACGGTGTTGCTG; R: AGCAGG CAAATCTCTCCAAAGT

HCN2-F: TCAACGAGGTGCTGGAGGA; R: CCTTGTGC AGGAGGATGGAA

HCN4-F: GACTGCTGGGTGTCCATCAA; R: AGAGCG CGTAGGAGTACTGCTT

Cav3-F: GCCCAGATCGTCAAGGAT; R: AGCAGCGTG GACAACAGA

Patch-clamp recordings

The experimental setup for patch-clamp recordings and data acquisition was similar to that described previously (Sartiani L, 2007 [4]; Bettiol E, 2007 [9]). Isolated cells were superfused by means of a temperature-controlled (37°C) microsuperfusor, allowing rapid changes of the solution. Patch-clamp pipettes, prepared from glass capillary tubes (Harvard Apparatus Ltd., www.harvardapparatus.com) by means of a 2-stage horizontal puller (P-87; Sutter Instrument) had a resistance of 2–3 MΩ when filled with the internal solution (see "Solutions and chemicals"). Series resistance (Rs) and membrane capacitance (Cm) were compensated to minimize the capacitive transient and routinely checked during the experiment. Only cells showing a stable Cm and Rs were included in the analysis. I_f current was measured in the whole-cell configuration by using appropriate external and pipette solutions (see "Solutions and chemicals"). From a holding potential of −40 mV, I_f was elicited by hyperpolarizing steps to −60/−140 mV and the current amplitude was measured as the difference between the instantaneous current at the beginning of the hyperpolarizing step and the steady-state current recorded at the end of the step.

Specific conductance was determined following the equation:

$$Gf = I/(V_m - V_{rev})$$

where Gf (pS pF^{-1}) is the conductance calculated at the membrane potential Vm (mV), I (pA pF^{-1}) the current density, and Vrev (mV), the reversal potential of the current. I_f specific conductance was normalized with respect to maximal conductance and values, expressed as mean ± SEM, were plotted versus membrane potential. Activation data were fitted by a Boltzmann function expressed by the equation:

$$g = gmax/\{1 + \exp[(V_{1/2} - V_m)/k]\},$$

where g is the conductance calculated at membrane potential Vm (mV), $V_{1/2}$ (mV) the fitted potential for half-maximal

activation, and k (mV) the slope factor describing the steepness of the activation curve.

Solutions and chemicals

The Kraft-Bruhe solution (mM) comprised glucose 20, creatine 5, taurine 5, EGTA 0.5, succinic acid 5, K_2-ATP 2, pyruvic acid 5, β-hydroxy-butyric acid 5, KCl 85, K_2HPO_4 $3H_2O$ 30, $MgSO_4$ $7H_2O$ 5, pH 7,1 with KOH.

The normal Tyrode solution (mM) comprised NaCl 140; KCl 5.4; $CaCl_2$ 1.8; $MgCl_2$ 1.2; D-glucose 10; Hepes 5, pH 7.35 with NaOH.

The modified Tyrode solution for I_f current was obtained from the normal Tyrode solution supplemented with (mM) $MnCl_2$ 2, $BaCl_2$ 2, and 4-aminopyridine 0.5 to eliminate Ca^{2+} current (T- and L-type), inward rectifier K^+ current, I_{K1}, and transient outward K^+ current, Ito, respectively. KCl was increased to 25 mM to amplify I_f. The pipette solution (mM) comprised K^+ aspartate 130; Na_2GTP 0.1; Na_2ATP 5; $MgCl_2$ 2; EGTA 11; $CaCl_2$ 5 (pCa 6.9); Hepes 10, pH 7.2 with KOH.

To deplete cholesterol, freshly isolated human atrial CM were resuspended in the Tyrode solution containing 200 μM $CaCl_2$ and incubated with 2 mM methyl-β-cyclodextrin (MβCD) (Sigma) for 90 min [10,11].

Results

HCN4 and Cav3 colocalize in hAV and hAA CM, but not in hF CM

As shown in Fig. 1A, B, HCN4, and Cav3 appear to be expressed across the whole cell surface membrane of hAA- and hAV-CM; colocalization can be inferred by the merging of the green and red channels in the same focal plane as shown by the yellow marking (*right panels* of A and B). HCN4 and Cav3 expression patterns in hF heart cells (hF-CM, ~12 weeks of age), were characterized by a spotted appearance across the cell membrane of both HCN4 and Cav3 (Fig. 1C; $n = 5$ independent experiments). Simultaneous expression of Cav3 and HCN4 in the same cells was inconsistent and colocalization was not observed in >99% of the cells examined, either when studied in individual cells (Fig. 1C) or in CM clusters (not shown).

Immunocytochemical analysis of hESC, hESC-CM, and HCN4-Cav3 colocalization

As expected from the previous demonstration of their functional presence [4], expression of the HCN4 protein was clearly detected in undifferentiated hESC; expression is

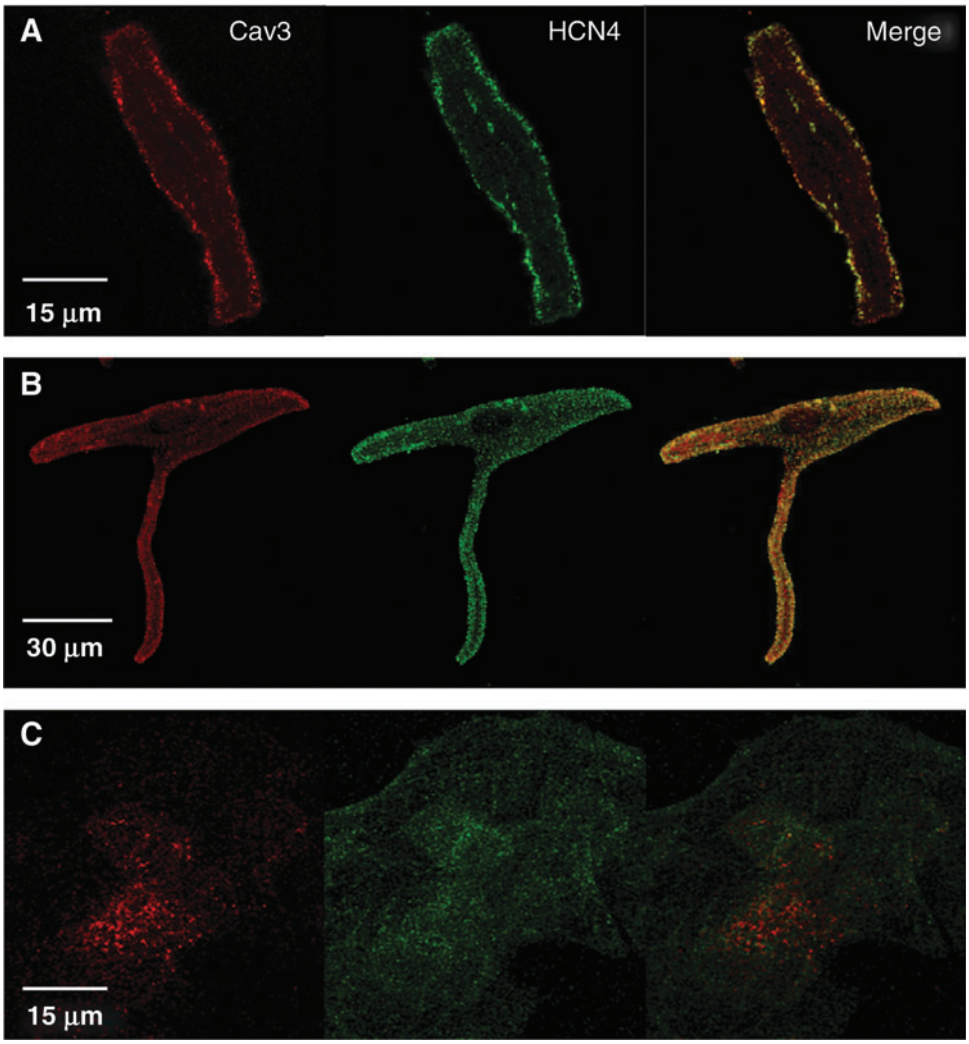

FIG. 1. Expression of hyperpolarization-activated cyclic nucleotide-gated channel (HCN)4 and Caveolin-3 (Cav3) in human adult and fetal cardiomyocytes (CM). Human adult ventricular (hAV) **(A)** and atrial (hAA) **(B)** CM expressing HCN4 (*green*) and Cav3 (*red*). Colocalization is observed upon merging (*yellow*). **(C)** Human fetal (hF) CM expressing HCN4 (*green*) and Cav3 (*red*). No colocalization is observed upon merging. Color images available online at www.liebertpub.com/scd

evident at the cell surface and characterized by a low-density pattern of expression with a spotted appearance across the membrane of the whole cell (Fig. 2A). Moreover, the expression of HCN4 in hESC, as examined using the 3D image reconstruction, clearly showed that the channels were localized mainly on the cell surface (Fig. 2B).Cav3 was absent in undifferentiated hESC.

Since both HCN4 and Cav3 appear to be expressed and colocalized across the whole-cell sarcolemma only in hAA- and hAV-CM (Fig. 1A, B), but not in undifferentiated hESC or hF-CM, we sought the time-course of this process in hESC-CM at different stages of maturation. To examine the expression and localization of HCN4 and Cav3 at the single cardiomyocyte level, whole beating hESC-CM clusters were fixed and stained immunocytochemically.

At d30, HCN4 had mainly a spotted appearance in hESC-CM (Fig. 3A, *white arrow*), similar to what was observed in undifferentiated hESC (Fig. 2A); however, the expression pattern varied within the cluster, as can be seen in Fig. 3A (*arrows*). Low expression of Cav3 was seen in ~20% of the cells of the cluster, localized also at the cell surface membrane ($n=3$ independent experiments). HCN4 and Cav3 were expressed in the same cells (Fig. 3A), but colocalization was absent, as suggested by the lack of yellow upon merging. A similar staining pattern was seen in hESC-CM at d60; however, Cav3 was expressed in ~50% of cells and with a greater density ($n=3$ independent experiments). Again, HCN4 and Cav3 were observed to be expressed in the same cells. Finally, and more interestingly, HCN4 and Cav3 were not only expressed in the same cells, but also colocalized in hESC-CM at d110; colocalization was never detected at any of the earlier stages of maturation. This pattern was observed in $n=3$ independent experiments. Expression of α-actinin was concurrently examined in HCN4-positive cells to confirm the cardiomyocytic nature of these cells (Fig. 3B). As HCN2 is also expressed in the heart and could contribute to f-current, we also examined its expression in relation to Cav3 at the same time points as were examined for HCN4. Expression of this HCN isoform did not change over time nor did it ever colocalize with Cav3 at any time point tested (Supplementary Fig. 1; Supplementary Data are available online at www.liebertonline.com/scd).

Immunohistochemical analysis of HCN4-Cav3 expression in hESC-CM and fetal heart

To preserve tissue structural integrity and the spatial relationship among cells, immunohistochemical staining was performed at d60 and d110 on consecutive sections to examine the expression of HCN4 and Cav3, as well as α-actinin. First, α-actinin was expressed in the beating clusters at both d60 and d110, which can be seen clearly in Fig. 4. Cav3 was also expressed at d60 and d110 through the cardiomyocyte (α-actinin-positive) portions of the clusters. Conversely, we could detect differential HCN4 expression within a single beating cluster, with some areas appearing to be more highly enriched than others. A general higher expression of HCN4 is observed at d60 in comparison to d110, where only a small section of the cluster contains cells expressing HCN4 in high density, as clearly shown in Fig. 4. Expression was compared to that found in fetal heart slices, where a clear-cut expression of each protein examined was observed (see Supplementary Fig. 2).

Transcriptional regulation of HCN4 and Cav3 in undifferentiated hESC and hESC-CM

As protein expression is regulated by different mechanisms in the cell, we assessed whether HCN4 and Cav3 are regulated at the transcriptional level during maturation. Thus, we manually isolated beating clusters of hESC-CM from hESC-derived EBs, at 3 time points (d30, d60, d110) and measured the mRNA expression of different HCN isoforms in these cells. Overall, mRNA expression of HCN and Cav3

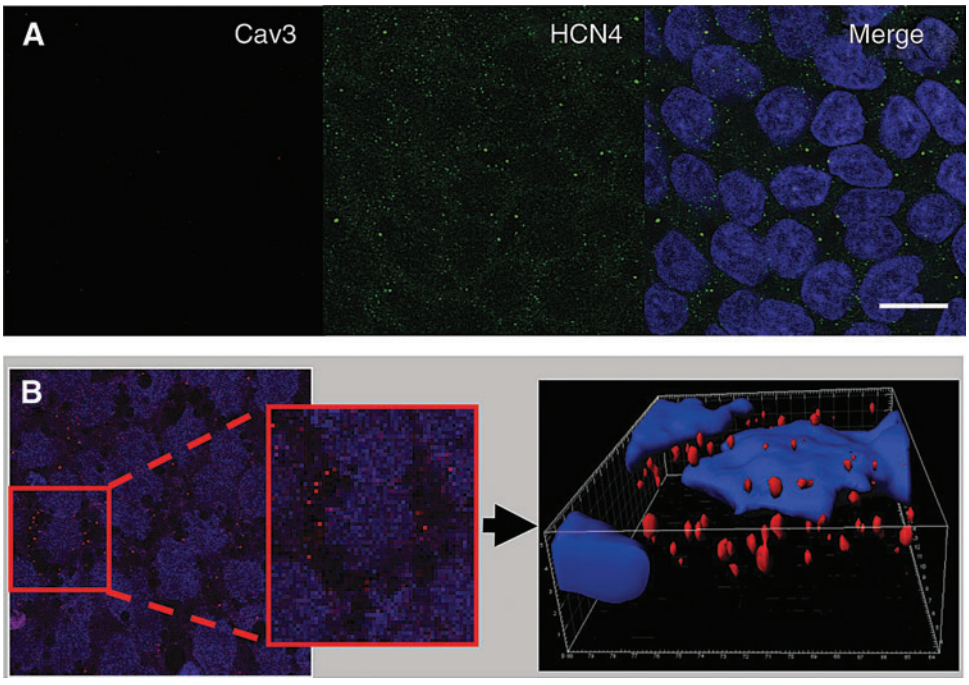

FIG. 2. Expression of HCN4 and Cav3 in undifferentiated human embryonic stem cell (hESC). **(A)** Undifferentiated hESC expressing HCN4 (*green*), but not Cav3. **(B)** 3D reconstruction of a stack of confocal images showing HCN4 expression (*red*) in a single undifferentiated hES cell, showing clearly the cell surface (sarcolemmal) localization of the ion channel. Scale bar = 10 μm. Color images available online at www.liebertpub.com/scd

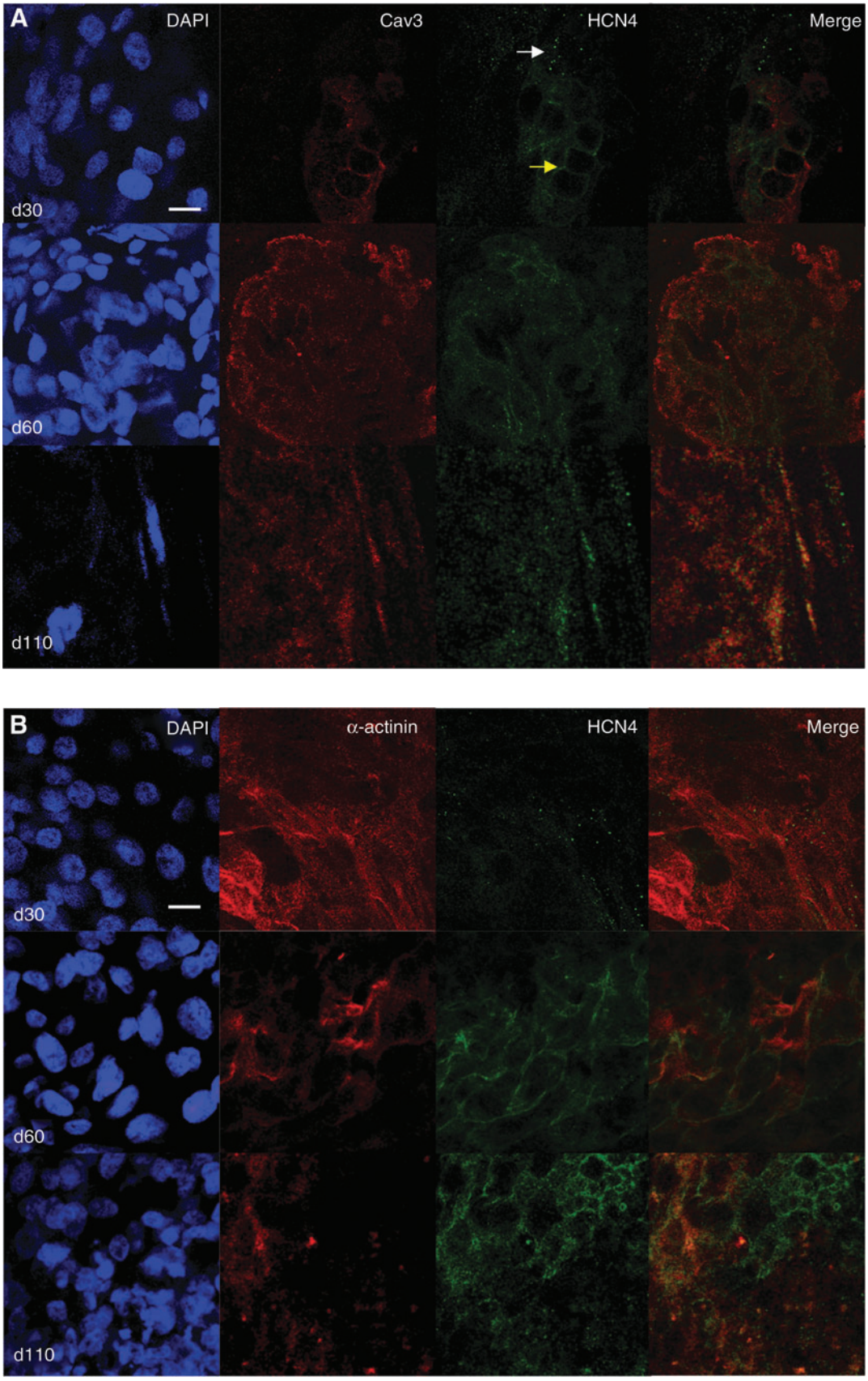

FIG. 3. Expression of Cav3, HCN4, and α-actinin in d30, d60, and d110 hESC-CM. **(A)** Cav3 and HCN4 double staining (d30: *white arrow* = low density; *yellow arrow* = high density) **(B)** α-actinin and HCN4 double staining to verify expression of HCN4 in cardiac-specific cells. Scale bar = 10 μm. Color images available online at www.liebertpub.com/scd

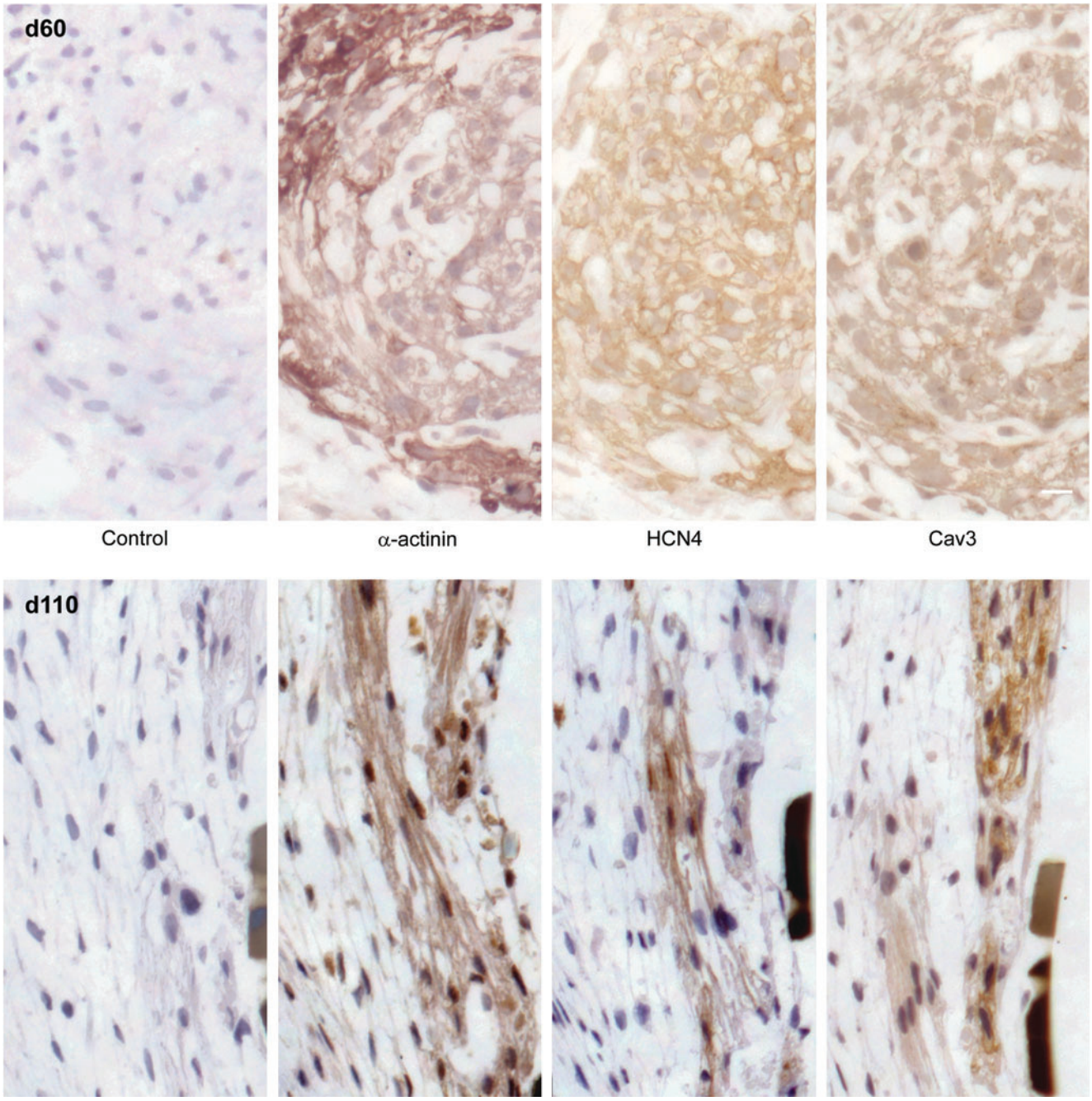

FIG. 4. Immunohistochemical (IHC) staining of whole hESC-CM clusters. IHC staining of hESC-CM at d60 and d110 with α-actinin, Cav3, and HCN4. Color images available online at www.liebertpub.com/scd

suggests major transcriptional regulation. In fact, we observed that HCN4 mRNA was highly expressed in undifferentiated hESC and in early CM (d30), in agreement with previous data from ours [4] and other laboratories [12,13], and decreased over time (d60 and d110) (Fig. 5). HCN1 and HCN2 were also expressed in undifferentiated hESC (d0); HCN1 also decreased over time upon maturation, whereas HCN2 expression remained relatively constant (Supplementary Fig. 3). Cav3 on the other hand, was not expressed in undifferentiated hESC (d0); it was clearly expressed at d60, and dramatically increased at d110, in agreement with our ICC findings.

Functional consequences of developmental changes in HCN4/Cav3 expression and localization

Figure 6 (A–E) shows typical I_f recordings obtained from hESC-CM at d60 and d110, hF-, hAA-, and hAV-CM. Currents exhibited different activation kinetics likely reflecting diverse isoform distribution, as previously reported by our and other laboratories [4,14]. When examining the voltage dependence (Fig. 6F), the potential of half-maximal activation (I_f $V_{1/2}$) for hAA-CM and hAV-CM were shifted leftward by about −20 and −10 mV, respectively, in comparison to hF-CM (hAA-CM:$V_{1/2} = -101.5 \pm 4.1$ mV, $n = 3$;

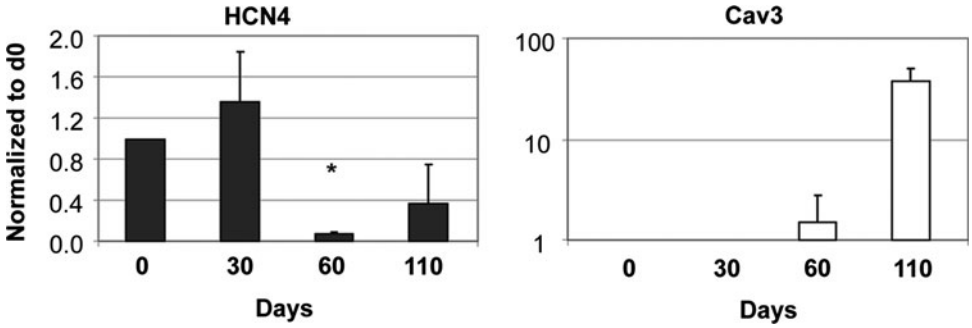

FIG. 5. Transcriptional regulation of HCN4 and Cav3 in undifferentiated hESC and hESC-CM. Real time PCR data for the expression of HCN4 and Cav3 in hESC-CM over time (*$P < 0.05$).

hAV-CM:$V_{1/2} = -94.4 \pm 1.7$ mV, $n = 6$; and hF-CM$V_{1/2} = 82.3 \pm 1.96$, $n = 11$). Interestingly, a similar difference of I_f voltage dependence was detected between hESC-CM at d100 (-96.8 ± 5.9 mV, $n = 6$) and hESC-CM at d60 (-83.2 ± 6.9 mV, $n = 8$). This modification turns into different I_f fractional activations at physiological resting potentials (e.g., -90 mV, for ventricular cells). In fact, in hESC-CM at d60, 65% ± 12% ($n = 8$) of the current was activated with respect to 30% ± 0.14% ($n = 6$, $P < 0.05$) in hESC-CM at d100, a value resembling what was observed in hAA-CM (0.34 ± 0.07, $n = 3$) and hAV-CM (0.39 ± 0.06, $n = 6$).

Caveolae disruption changes the properties of I_f current expressed in human adult CM

Previous data suggest that HCN4-Cav3 colocalization has relevant functional consequences in rodent SAN cells [2], namely, on voltage-dependent activation. We tested whether

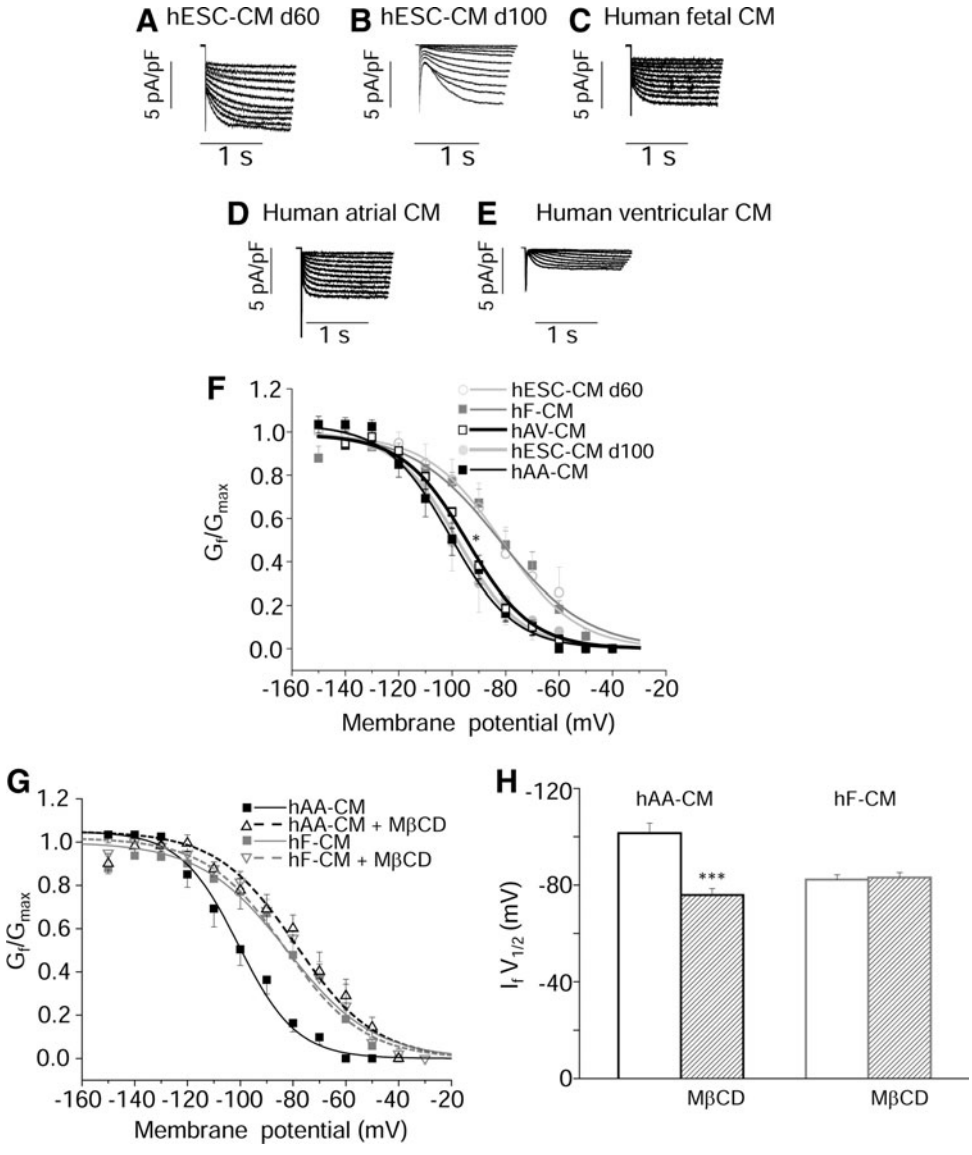

FIG. 6. Cardiomyocyte electrophysiological recordings. **(A–E)** Representative I_f current traces in hESC-CM (60 and 100 days), hF-CM and hAA- and hAV-CM. **(F)** Activation curves of I_f current for each cell type (*$P < 0.05$). **(G)** Effects of membrane cholesterol depletion on activation properties of f-channels in hAA-CM ($n = 3$) and hF-CM ($n = 6$). **(H)** Bar graph showing mean potential (±SEM) of half maximal activation of f-current (I_f $V_{1/2}$) in hAA-CM and hF-CM, treated or not with methyl-β-cyclodextrin (MβCD). ***$P < 0.001$.

such property also holds true for Cav3 expressed in human CM. Therefore, we disrupted the caveolar compartment of CM by depleting membrane cholesterol with MβCD and examined their activation properties. Using isolated hAA CM, which represent the best eligible cell population in our experimental setting, we found that hAA-CM incubated with or without MβCD, resulted in a shift of +25 mV of I_f $V_{1/2}$ (from -101.5 ± 4.1 to -75.9 ± 2.7 mV, $n=3$, $P<0.001$) (Fig. 6G). Of note, the latter value was not statistically different from that of hF-CM (-82.3 ± 1.96 mV, $n=11$; Fig. 6 F–H). Finally, we assessed the consequence of treatment with MβCD on hF-CM and demonstrated that voltage-dependence of f-channel activation remained completely unaffected by the treatment ($V_{1/2}$ -83.1 ± 2.1 mV; Fig. 6G, H).Therefore, disruption of caveolae, and thus, disruption of Cav3-f-channel colocalization, resulted in the regression of $I_f$voltage dependence toward values measured in immature fetal CM (hF-CMs), also becoming similar to that of hESC-CM at d60.

Discussion

In the present study, we have investigated the expression and localization of HCN4 and Cav3 in CM derived from hAA and hAV heart, hF heart, as well as in hESC-CM at different stages of development/maturation. Here we demonstrate that the presence, and more specifically the colocalization, of Cav3 in cells highly expressing HCN4 represents a crucial step of cardiac maturation, which modifies channel activation properties. Due to the role of I_f, that is, the HCN-mediated ion current on diastolic membrane potential, developmental changes in channel compartmentalization and association to Cav3 may have functional relevance on basal cell physiology and contribute to the progression toward the adult cardiac phenotype.

Membranous lipid rafts enriched in caveolae are known to influence the function of many different cardiac ion channels, which has been well reviewed by Dart [15]. It has been previously shown that HCN4 associates with Cav3 in mouse and rabbit SAN cells [2,16], where the association regulates channel activation properties and responsiveness to adrenergic modulation [17]. This HCN4-Cav3 association has been previously inferred for the human versions of these proteins on the basis of co-immunoprecipitation experiments in human HEK293 cells stably expressing HCN4 channels and Cav3 [18]. Here we directly demonstrate that indeed HCN4 and Cav3 are present and colocalize in native human adult, but not fetal, CM, with a cell surface membrane pattern of expression (Fig. 1). These different patterns in fetal versus adult myocytes suggest that acquisition of a precise sarcolemmal organization of ion channels occurs in a development-dependent fashion: indeed, in undifferentiated hESC, HCN4, but not Cav3, is present and functionally active. We have found that in hESC-CM, HCN4-Cav3 association is dependent on the stage of cardiomyocyte maturation (Figs. 1, 3, and 5), a clear colocalization being consistently present only in late hESC-CM (d110), but not before. We suggest that this developmental event may represent a crucial step in cardiac maturation leading to caveolar localization of the HCN4 channel, similar to that present in native human atrial and ventricular cells.

Functional consequences of this phenomenon have been assessed in hAA CM, which provided evidence of a positive shift of the I_f current voltage dependence upon caveolar disruption, in accordance with data obtained from rabbit SAN cells [2,17]. Of note, after caveolar disruption, the I_f activation curve generated for hAA CM was not statistically different from that of hF-CM, suggesting that when the f-channel is lacking interaction with Cav3, its activation properties are similar to those seen in fetal CM. This hypothesis is further re-enforced considering the consequence of caveolar disruption on the f-channel in hF-CM, which remained completely unaffected by treatment (Fig. 6G, H). This is in accordance with a lack of colocalization of Cav3 and HCN4 (Fig. 1C). On the other hand, midpoint activation voltage of I_f lies around -95 mV in adult atrial and ventricular CM (when caveolae are intact) and in late hESC-CM (d100). The latter, while sharing most of the properties of the adult, native CM and despite their inherent limitations, have an ICC and histochemical profile revealing high Cav3 expression and colocalization with HCN4 compared to d60 hESC-CM. Altogether, these data suggest that in human CM, developmental changes from the fetal to adult phenotype are associated with (1) a leftward shift of voltage activation, and (2) a sensitivity to MβCD treatment (disruption of I_f-Cav3 association). Data from immunofluorescence experiments and patch-clamp recordings allow us to infer that hESC-CM in vitro recapitulate this process, and lead us to hypothesize that a similar developmental change in HCN4-Cav3 association occurs in hESC-CM, which accounts for the modification of f-current described between the early ($\approx$60-days) and late ($\approx$110 days) developmental window.

At earlier stages (d60 hESC-CM) and in fetal CM, the lack of HCN4-Cav3 colocalization and a more positive activation voltage of I_f go hand-in-hand. Of note, the lack of quantitative modifications of the HCN transcript during the time span considered for the electrophysiological analysis (from 60 to 100 days of differentiation) reasonably excludes a contribution of the isoform variation to the shift of the I_f activation curve. Altogether, these data support the hypothesis that during maturation, HCN4—a major isoform coding for f-channels in the human heart—is recruited into caveolar compartments and interact with the Cav3 protein. By contrast, HCN2 maintains the similar and constant expression found in undifferentiated cells, with no colocalization with the Cav3 protein upon maturation. Since different HCN subunits are reported to combine in the same protein complex forming either heterotetramers or homotetramers [19], our data suggest the existence of HCN2 homotetramers in hESC-CM; however, despite this, we cannot exclude the formation of heterotetramers at a different developmental stage (i.e., beyond 100 days of differentiation) or in a minority of CM in the developmental stages investigated in the present study.

At variance with what is known about native SAN cells [2,16,17], the functional significance of HCN4-Cav3 colocalization in hESC-CM in terms of modulation exerted by autonomic stimuli is unknown and remains to be established. However, it is worth noting that beta-adrenergic stimulation positively modulates I_f activation only in late, but not in early hESC-CM [4], suggesting that channel responsiveness to adrenergic signaling is acquired when the channel is localized into the caveolar compartment. Similarly, to adult cardiac myocytes [20], we hypothesize that in late hESC-CM, adrenergic receptors and HCN4 channels likely cluster in

close proximity, such as in the caveolar compartment, thereby allowing an effective functional coupling.

In the adult heart, HCN4/I_f is abundant in SAN and subsidiary pacemaker cells, identified by the presence of a clear-cut diastolic depolarization phase of the action potential. In this line, the hypothesis of a progressive clustering of HCN4 channels into caveolae and the interaction with the Cav3 protein during maturation of hESC-CM fully agrees with our previous data demonstrating that the frequency of spontaneous action potentials and the rate of the diastolic depolarization phase slows down during hESC-CM maturation [4,21].

In undifferentiated hESC, detection of I_f in cells is present, but rare (only measurable in around 10% of cells), but when present, the current density is remarkable (1.2 ± 0.3 pA/pF at -120 mV). This observation is in line with the appearance of a spotted and faint signal of the HCN4 protein observed in immunofluorescence images (Fig. 2).The functional relevance of HCN4/I_f in undifferentiated hESC is currently unknown and further research is needed to understand the possible significance of this channel in early human development. Interestingly, a recent study [22] suggests a role of the HCN channel on proliferation and cell cycle progression of the mouse ESC. Whether a similar function takes place in the human ESC is an intriguing speculation that deserves further investigation.

The present study may have possible implications for cardiac pathology, such as hypertrophy and failure. Indeed, it is well established that several modifications occur at functional and molecular levels in cardiac myocytes, a phenomenon known as cardiac cellular remodeling that may underlie the increased propensity of cardiac tissue to develop arrhythmias. Mounting data demonstrate that cardiac remodeling originates from a fetal pattern of genes, which are re-expressed during the diseased state. I_f current gain-of-function joined to HCN overexpression is an integral part of this pattern, as assessed in animal and human diseased ventricular myocytes [5,6]. In this context, acquisition of I_f current has been proposed as a mechanism contributing to the increased propensity to develop arrhythmias [23]. The regression toward a fetal phenotype in this disease state opens the question of whether a disruption of the HCN4-Cav3 protein interaction takes place in this context. Indeed, a positive shift of the I_f activation curve has been observed in CM from diseased human hearts [24]. Finally, perturbations in the expression and/or function of HCN4 in humans have been shown to elicit arrhythmias and chronotropic disruptions [25–28], indicating the importance of the correct expression and function of this ion channel in the heart.

Conclusions

Our work shows for the first time that expression of Cav3, a crucial component of cardiac sarcolemma, increases during development in vitro in hESC-CM. At the same time, colocalization with HCN4, whose functional and molecular expression is detected in hESC before commitment and differentiation toward the cardiac phenotype, contributes to attainment of the adult-like biophysical properties of the HCN-mediated current, I_f.

Acknowledgments

Authors wish to thank Dr. Gabriella Vannelli (the University of Florence, Italy) and Marie Cohen (Geneva University Hospitals) for providing human fetal hearts and helpful advice on tissue handling and processing, and Dr. Tommaso Mello (the University of Florence, Italy) for assistance in confocal microscopy. This study was supported by grants from the Italian MIUR (PRIN 2007AL2YNC) and from EnteCassa di Risparmio di Firenze (EC), and by the Swiss National Science Foundation (grant #310031-110002(MJ)) and the FondsGerbex-Bourget CGR82102 of the Geneva University Hospitals (MJ).

Author Disclosure Statement

No competing financial interests exist.

References

1. Balijepalli RC and TJ Kamp. (2008). Caveolae, ion channels and cardiac arrhythmias. Prog Biophys Mol Biol 98:149–160.
2. Barbuti A, B Gravante, M Riolfo, R Milanesi, B Terragni and D DiFrancesco. (2004). Localization of pacemaker channels in lipid rafts regulates channel kinetics. Circ Res 94:1325–1331.
3. Barbuti A, A Scavone, N Mazzocchi, B Terragni, M Baruscotti and D Difrancesco. (2012). A caveolin-binding domain in the HCN4 channels mediates functional interaction with caveolin proteins. J Mol Cell Cardiol 53:187–195.
4. Sartiani L, E Bettiol, F Stillitano, A Mugelli, E Cerbai and ME Jaconi. (2007). Developmental changes in cardiomyocytes differentiated from human embryonic stem cells: a molecular and electrophysiological approach. Stem Cells 25:1136–1144.
5. Cerbai E and A Mugelli. (2006). I(f) in non-pacemaker cells: role and pharmacological implications. Pharmacol Res 53: 416–423.
6. Sartiani L, E Cerbai and A Mugelli. (2011). The funny current in cardiac non-pacemaker cells: functional role and pharmacological modulation. In: *Modern Pacemakers—Present and Future*. Das MK, ed. InTech: Rijeka, Croatia.
7. Xu C, S Police, N Rao and MK Carpenter. (2002). Characterization and enrichment of cardiomyocytes derived from human embryonic stem cells. Circ Res 91:501–508.
8. Lonardo G, E Cerbai, S Casini, G Giunti, M Bonacchi, F Battaglia, B Fiorani, PL Stefano, G Sani and A Mugelli. (2004). Atrial natriuretic peptide modulates the hyperpolarization-activated current (If) in human atrial myocytes. Cardiovasc Res 63:528–536.
9. Bettiol E, L Sartiani, L Chicha, KH Krause, E Cerbai and ME Jaconi. (2007). Fetal bovine serum enables cardiac differentiation of human embryonic stem cells. Differentiation 75: 669–681.
10. Ohtani Y, T Irie, K Uekama, K Fukunaga and J Pitha. (1989). Differential effects of alpha-, beta- and gamma-cyclodextrins on human erythrocytes. Eur J Biochem 186:17–22.
11. Kilsdonk EP, PG Yancey, GW Stoudt, FW Bangerter, WJ Johnson, MC Phillips and GH Rothblat. (1995). Cellular cholesterol efflux mediated by cyclodextrins. J Biol Chem 270:17250–17256.
12. Kim C, M Majdi, P Xia, KA Wei, M Talantova, S Spiering, B Nelson, M Mercola and HS Chen. (2010). Non-cardiomyocytes influence the electrophysiological maturation of human embryonic stem cell-derived cardiomyocytes during differentiation. Stem Cells Dev 19:783–795.
13. Zhu WZ, Y Xie, KW Moyes, JD Gold, B Askari and MA Laflamme. (2010). Neuregulin/ErbB signaling regulates cardiac subtype specification in differentiating human embryonic stem cells. Circ Res 107:776–786.

14. Stillitano F, G Lonardo, S Zicha, A Varro, E Cerbai, A Mugelli and S Nattel. (2008). Molecular basis of funny current (If) in normal and failing human heart. J Mol Cell Cardiol 45:289–299.
15. Dart C. (2010). Lipid microdomains and the regulation of ion channel function. J Physiol 588:3169–3178.
16. Brioschi C, S Micheloni, JO Tellez, G Pisoni, R Longhi, P Moroni, R Billeter, A Barbuti, H Dobrzynski, et al. (2009). Distribution of the pacemaker HCN4 channel mRNA and protein in the rabbit sinoatrial node. J Mol Cell Cardiol 47:221–227.
17. Barbuti A, B Terragni, C Brioschi and D DiFrancesco. (2007). Localization of f-channels to caveolae mediates specific beta2-adrenergic receptor modulation of rate in sinoatrial myocytes. J Mol Cell Cardiol 42:71–78.
18. Ye B, RC Balijepalli, JD Foell, S Kroboth, Q Ye, YH Luo and NQ Shi. (2008). Caveolin-3 associates with and affects the function of hyperpolarization-activated cyclic nucleotide-gated channel 4. Biochemistry 47:12312–12318.
19. Biel M, C Wahl-Schott, S Michalakis and X Zong. (2009). Hyperpolarization-activated cation channels: from genes to function. Physiol Rev 89:847–885.
20. Nikolaev VO, A Moshkov, AR Lyon, M Miragoli, P Novak, H Paur, MJ Lohse, YE Korchev, SE Harding and J Gorelik. (2010). Beta2-adrenergic receptor redistribution in heart failure changes cAMP compartmentation. Science 327: 1653–1657.
21. Paci M, L Sartiani, M Del Lungo, M Jaconi, A Mugelli, E Cerbai and S Severi. (2012). Mathematical modelling of the action potential of human embryonic stem cell derived cardiomyocytes. Biomed Eng Online 11:61.
22. Lau YT, CK Wong, J Luo, LH Leung, PF Tsang, ZX Bian and SY Tsang. (2011). Effects of hyperpolarization-activated cyclic nucleotide-gated (HCN) channel blockers on the proliferation and cell cycle progression of embryonic stem cells. Pflugers Arch 461:191–202.
23. Teerlink JR. (2010). Ivabradine in heart failure—no paradigm SHIFT…yet. Lancet 376:847–849.
24. Cerbai E, L Sartiani, P DePaoli, R Pino, M Maccherini, F Bizzarri, F DiCiolla, G Davoli, G Sani and A Mugelli. (2001). The properties of the pacemaker current I(F)in human ventricular myocytes are modulated by cardiac disease. J Mol Cell Cardiol 33:441–448.
25. Schulze-Bahr E, A Neu, P Friederich, UB Kaupp, G Breithardt, O Pongs and D Isbrandt. (2003). Pacemaker channel dysfunction in a patient with sinus node disease. J Clin Invest 111:1537–1545.
26. Ueda K, Y Hirano, Y Higashiuesato, Y Aizawa, T Hayashi, N Inagaki, T Tana, Y Ohya, S Takishita, et al. (2009). Role of HCN4 channel in preventing ventricular arrhythmia. J Hum Genet 54:115–121.
27. Nof E, D Luria, D Brass, D Marek, H Lahat, H Reznik-Wolf, E Pras, N Dascal, M Eldar and M Glikson. (2007). Point mutation in the HCN4 cardiac ion channel pore affecting synthesis, trafficking, and functional expression is associated with familial asymptomatic sinus bradycardia. Circulation 116:463–470.
28. Baruscotti M, A Bucchi, C Viscomi, G Mandelli, G Consalez, T Gnecchi-Rusconi, N Montano, KR Casali, S Micheloni, A Barbuti and D DiFrancesco. (2011). Deep bradycardia and heart block caused by inducible cardiac-specific knockout of the pacemaker channel gene Hcn4. Proc Natl Acad Sci U S A 108:1705–1710.

Address correspondence to:
Prof. Elisabetta Cerbai
Centro Interuniversitario di Medicina Molecolare e Biofisica Applicata (CIMMBA)
University of Firenze
Viale Pieraccini 6
50139 Firenze
Italy

E-mail: elisabetta.cerbai@unifi.it

Received for publication May 9, 2012
Accepted after revision January 10, 2013
Prepublished on Liebert Instant Online January 11, 2013